APPENDIX I

pH AMENDMENT EVALUATION

I.1 CAP pH MODEL MEMO

I.2 SIDERITE LEACHATE EVALUATION

I.1

CAP pH MODEL MEMO

S.S. PAPADOPULOS & ASSOCIATES, INC.
Environmental & Water-Resource Consultants

Memorandum

Date:	December 3, 2009
From:	Dimitri Vlassopoulos, Brad Bessinger, and Jessica Goin
To:	David Smith, Ed Glaza (Parsons)
Project:	Onondaga Lake
Subject:	**ILWD Porewater pH Neutralization Geochemical Modeling Study**

This memorandum present the results of a modeling study conducted by SS Papadopulos & Associates (SSPA) to evaluate options for incorporating a chemical amendment to a sediment cap for porewater pH control in areas containing hyperalkaline in-lake waste deposits (ILWD) at Onondaga Lake. Amendment for pH control is being considered for enhancement of biological decay within the chemical isolation layer of the ILWD cap. Previous laboratory investigations evaluated several potential amendments and concluded that siderite (natural iron carbonate) was the most suitable amendment for application in a subaqueous sediment cap (SSPA, 2009). Here, we (1) develop a kinetic/equilibrium geochemical reactive transport model to describe porewater pH neutralization within a sediment cap by siderite amendments, (2) calibrate the kinetic model parameters to pH-time evolution curves measured in batch tests, and (3) apply the model to evaluate the minimum required application rate and amended layer thickness to ensure effective porewater pH neutralization for the cap design lifetime.

This memorandum is organized into four sections. Section 1 reviews the batch test methods and results as they pertain to the development of a predictive geochemical model. Section 2 describes the geochemical kinetic model development and calibration. Section 3 presents results from long-term simulations of pH neutralization under field conditions. Finally, Section 4 discusses uncertainty in model predictions and proposes laboratory column tests be conducted in order to confirm pH neutralizing performance within the sediment cap under dynamic conditions.

1 Summary of Batch Test Results

As described in SSPA (2009), a series of laboratory batch tests were conducted to measure the kinetics of hyperalkaline porewater pH (~12) neutralization by siderite. Batch tests were performed over a wide range of liquid to solid-amendment (L/S) ratios with hyperalkaline porewater retrieved from site TR-03A in SMU-1. Three forms of siderite were tested:

- Siderite, powdered: A fine orange to tan powder supplied by Prince Agri. This is a mined mineral that is used primarily as an iron supplement for livestock. It consists of 77% iron carbonate, 12% quartz, 10% clay, and minor pyrite.

- Siderite, pelletized: A brown, pea-gravel material manufactured from powdered siderite using a calcium aluminate binder supplied by Chemical Products Industries. It consists of 73% iron carbonate, 22% quartz, and minor clay, calcite, and goethite.

- Siderite, granular: A light brown-to-gray, gravelly material from a mine in East Texas supplied by Sidco Minerals Inc. It consists of 76% iron carbonate, 12% quartz, 11% kaolinite, and 2% goethite.

Powdered siderite and pelletized siderite were used as received. Granular siderite was also used as received by additionally size-fractionated to examine the effect of grain size on reactivity. The experimental conditions used in each experiment (including siderite type, L/S ratio, and porewater used) are summarized in Table 1. Initial batch tests conducted with as-received material showed much higher reactivity at early times, which was attributed to the presence of extremely fine siderite particles adhering on the larger grains (SSPA, 2009). To ensure data would be representative of the performance of the bulk material, pelletized siderite and granular siderite were pre-rinsed in distilled water to remove fines prior to all subsequent tests. In each batch test, porewater pH was monitored as a function of time until a pH of 8 or less was reached. The measured pH evolution curves were used to calibrate the geochemical kinetic model discussed below.

2 Kinetic Model of pH Neutralization by Siderite

A geochemical kinetic model was developed to quantitatively simulate the process of porewater pH neutralization by siderite. The objective of the modeling was to provide a tool for predicting the long-term performance and evolution of porewater pH within a siderite-amended sediment cap. Reactions were formulated based on current knowledge of dissolution and precipitation of carbonate minerals. Rate constants for dissolution and precipitation reactions were calibrated with the batch test data.

Three principal chemical reactions were considered to be involved in the pH neutralization process. The first is the dissolution of siderite which releases iron and carbonate ions:

$$FeCO_{3(s)} = Fe^{2+} + CO_3^{2-} \quad (1)$$

Second, the reaction of dissolved iron with hydroxyl (OH^-) ions and subsequent precipitation of hydrous iron oxide (e.g. goethite) removes OH^- from solution, thereby lowering pH:

$$Fe^{2+} + 3OH^- = FeOOH_{(s)} + H_2O + e^- \quad (2)$$

Reaction (2) represents the net reaction of iron hydrolysis, oxidation and precipitation. The actual process is more complex and proceeds through a series of reactions in which metastable amorphous iron hydroxides (e.g. $Fe(OH)_3$) will form initially and be converted to the thermodynamically more stable goethite over time. The stoichiometry of the net reaction: 3 moles OH- neutralized per mole of Fe dissolved, however, is unaffected by aging of the iron oxide precipitates, as aging of precipitates primarily involves a dehydration reaction. The electron (e^-) produced from the oxidation of Fe^{2+} in reaction (2) indicates that formation of goethite (or other iron oxides) from dissolution of siderite is a redox-dependent process that may require additional electron acceptors to facilitate the oxidation of iron. However, measured Eh and pH measurements of ILWD porewaters (SSPA, 2008) show that redox conditions are already within the stability field of goethite (Figure 1). Therefore, suitable conditions for the spontaneous precipitation of goethite (or similar iron oxide precursors) via reaction (2) already exist under the anaerobic conditions that characterize the ILWD deposits. Additional electron acceptors such as dissolved oxygen are therefore not required for iron oxides to form. As the porewater pH decreases due to the formation of iron oxides, the electrons produced will drive the system Eh to values buffered by iron oxide-porewater equilibrium.

Third, the accumulation of dissolved carbonate species from siderite dissolution leads to precipitation of calcite from the calcium-rich porewater solution:

$$Ca^{2+} + CO_3^{2-} = CaCO_{3(s)} \quad (3)$$

The overall rate of neutralization of porewater pH will depend on the rates of the three reactions described above. More precisely, it will depend on the slowest of these three reactions as that will be the rate-determining step for the overall process. Furthermore, the rate-determining step may change due to the changing solution chemical composition over time as siderite dissolves, such that the overall process kinetics is nonlinear in time. Because siderite dissolution and calcite precipitation are both slow processes (Pokrovsky and Schott 2002; Lebron and Suarez 1996), these reactions were modeled using kinetic rate expressions. Goethite precipitation, on the other hand, was modeled as an instantaneous (equilibrium) reaction, consistent with the

observed rapid development of orange-brown precipitates in the siderite batch test jars (SSPA, 2009).

2.1 Reaction Kinetics Formulation

The rate of dissolution of siderite under the batch test conditions can be described as the sum of two mechanisms:

$$\frac{dm_s}{dt} = \left(k_s + k_{sb} a_{H^+}^{n_b}\right) \times m_s \times (1 - \Omega_s) \qquad (4)$$

where dm_s/dt is the overall rate of siderite dissolution [moles second^{-1}], k_s is the rate constant for the pH-independent dissolution mechanism [moles gram^{-1} second^{-1}], k_{sb} is the rate constant for the pH-dependent dissolution mechanism [moles gram^{-1} second^{-1}] which contributes at high pH[1], a_{H^+} is the proton activity (pH = $-log\, a_{H^+}$), the exponent n_b is the order of the reaction mechanism with respect to proton activity, m_s [grams] is the mass of siderite in the system, and Ω_s is the degree of saturation of porewater with respect to siderite. This formulation is mathematically consistent with current models of carbonate mineral dissolution kinetics (Pokrovsky and Schott, 2002; Duckworth and Martin, 2004; Palandri and Kharaka, 2004; Schott et al, 2009).

The rate expression for calcite precipitation is based on the formulation of Morse et al. (2007):

$$\frac{dm_c}{dt} = k_c \times (\Omega_c - 1)^{n_c} \qquad (5)$$

where dm_c/dt is the rate of calcite precipitation [moles second^{-1}], k_c is the calcite precipitation rate constant (moles second^{-1}), Ω_c is the degree of saturation of porewater with respect to calcite, and n_c is an exponent relating the dependence of the reaction rate to the degree of saturation. Unlike equation (4), there is no mass-dependent term in this expression. Instead, the rate of calcite precipitation is described by a single empirical rate constant that implicitly includes the effects of mass-dependent reactive surface area on calcite nucleation and growth. This assumption is reasonable given that calcite is one of the most abundant mineral phases identified in samples of ILWD (SSPA, 2008b), and porewater solutions are generally slightly supersaturated with respect to calcite.

[1] Schott et al. (2009) recently reviewed a large body of experimental data on the dissolution rates of carbonate minerals and discussed evidence for enhanced dissolution rates at high pH. The increased dissolution rates at high pH are attributed to a reaction mechanism between hydroxyl ions and negatively charged surface metal oxo groups (i.e. >FeO$^-$ on siderite) whose surface concentration increases with increasing pH. The k_{sb} term was thus included in equation (4) to capture the observed high pH behavior.

2.2 Kinetic Model Calibration

The statistical parameter optimization program PhreePlot (Kinniburgh and Cooper, 2009) was used to calibrate the model parameters k_s, k_{sb}, k_c, and n_c in equations (4) and (5) by fitting the porewater pH evolution curves. PhreePlot combines PHREEQC[2] (Parkhurst and Appelo, 1999) with a nonlinear fitting subroutine that minimizes the weighted sum of squares of residuals between observed and predicted pH values. The initial value for m_s (equation 4) was based on the amount of iron carbonate (siderite) in the bulk amendment used in each batch experiment. A value of -1 was used for the exponent n_b, which is within the range shown to replicate carbonate mineral dissolution under alkaline conditions (Schott et al, 2009). The initial solution chemistry was defined from chemical analyses of porewaters used in the batch tests as reported in SSPA (2009). The saturation parameters Ω_s and Ω_c for siderite and calcite, respectively were computed within PhreePlot from the modeled solution composition at each time step.

Initial evaluations of data from batch tests conducted with unrinsed powdered siderite and pelletized siderite indicated that the model could not provide a satisfactory fit to the initial drop in porewater pH observed during the first 24 hours of reaction. We hypothesized that this sharp pH drop at early time was due to the dissolution of extremely fine dust particles that adhere to the larger grains, and are more reactive than the bulk material due to their higher specific surface area. The presence of a "fines" fraction in powdered, pelletized, and granular siderite was confirmed by observation (when rinsing the raw material in water, the water became turbid). Subsequently, all pelletized and granular siderite amendments were thoroughly rinsed with distilled water prior to batch testing in order to remove the fines.

[2] PHREEQC is a USGS-supported geochemical modeling software that is capable of simulating a wide range of geochemical processes. The code uses a thermodynamic database and a chemical description of solid and aqueous phases determined through laboratory analysis to predict solution pH and the distribution of chemical components between solid, aqueous, and gaseous phases. PHREEQC is based on chemical thermodynamics and the energetics of possible chemical reactions are supplied to the program through the thermodynamic database. PHREEQC uses this information, along with the total elemental compositions of the system being modeled, to minimize the overall energy of the system subject to any additional constraints. PHREEQC simultaneously solves expressions relating the mass of each element to its distribution between different forms (mass balance equations), expressions representing the Gibbs free energy change of prescribed reactions (mass action equations), and an expression for electrical neutrality (the charge balance equation). PHREEQC can simulate several types of geochemical processes, including aqueous phase reactions, ion exchange reactions, surface complexation reactions, and mineral precipitation and dissolution reactions. Reactions can be represented as either equilibrium or kinetically controlled.

In order to achieve a better fit to the pH evolution curves for the powdered and unrinsed pelletized siderite batch tests, equation (4) was modified to include a term for the dissolution of a siderite "fines" fraction:

$$\frac{dm_s}{dt} = \left\{\left(k_s + k_{sb} a_{H^+}^{n_b}\right) \times (m_s - m_{sf}) + k_{sf} m_{sf}\right\} \times (1 - \Omega_s) \qquad (6)$$

where k_{sf} is the rate constant for highly-reactive siderite fines [moles gram^{-1} second^{-1}], and m_{sf} is the mass of siderite "fines" present. These two additional parameters were optimized for fits to batch tests with powdered and unrinsed pelletized siderite.

2.3 Model Calibration Results

The optimized kinetic parameters obtained from the fits to the experimental pH evolution curves are summarized in Table 2, and Figures 2 to 4 compare measured and simulated pH as a function of time. For fitting purposes, batch test data for replicate tests using unrinsed siderite were grouped together.

As shown in Table 2, dissolution rate constants (k_s) are generally higher by as much as 1 to 2 orders of magnitude for siderite powder than either pelletized or granular siderite. These results reflect the higher reactive surface area of the powder relative to the coarser varieties.

The variability in dissolution rate constants determined for granular siderite is also expected to be related to reactive surface area. Although the rate constants for granular siderite generally increase with decreasing grain size fraction for a given L/S ratio (Figures 5a and 5b), there are deviations from the expected trend which suggest that the abundance of crystal surface imperfections with higher reactivity, such as dislocations and kinks, may also control the rate of dissolution. The range of fitted rate constants for granular siderite batch tests is therefore due in part to surface area and in part to natural heterogeneity of the samples. Rate constants for bulk granular siderite dissolution vary by less than a factor of 20 for k_s and 3 for k_{sb}, which can be considered to represent the level of uncertainty due to heterogeneity. The rate of siderite dissolution is therefore much less sensitive to surface heterogeneity at high pH than at low pH.

3 Sediment Cap Porewater pH Model

This section presents the development and application of a geochemical model for the simulation of a siderite-amended sediment cap. The model can be used to estimate the minimum siderite application rate needed to ensure neutralization of porewater pH for the design lifetime of the

cap. The model is described and applied to evaluate amended cap performance under two scenarios – a 3-inch versus a 6-inch siderite-amended layer.

From constructability and laboratory performance standpoints, granular siderite is the preferred amendment form. Due to its fine grain size, siderite powder would likely be easily dispersed through the lake water column during placement, which could pose a significant challenge for delivery of a uniformly mixed amended layer. Pelletized siderite is a manufactured material that would be supplied at greater cost than granular siderite, with no perceived benefit from the calcium aluminate binder added during the manufacturing process. The fact that pelletized siderite showed the slowest pH neutralization rate indicates the binder may have a potentially detrimental effect.

3.1 Model Development

The sediment cap model was constructed using the geochemical reactive transport software PHREEQC (Parkhurst and Appelo 1999). PHREEQC is capable of performing reactive solute transport calculations in one-dimensional water-saturated porous media by solving a set of partial differential equations for flow and transport and a set of nonlinear algebraic and ordinary differential equations for chemistry. The equations that are solved numerically include: (1) the saturated porewater flow equation for conservation of total fluid mass, (2) a set of solute-transport equations for conservation of mass of each solute component of a chemical reaction system, and (3) a set of chemical reaction equations comprising mass balance equations, mass action equations, and kinetic rate equations. A finite-difference technique is used for the spatial and temporal discretization of the flow and transport equations.

The cap was represented by a 5-foot thick layer of quartz sand (with an assumed effective porosity of 0.3) emplaced directly on top of ILWD (Figure 6) containing a siderite-amended layer at its base (thickness of 3 or 6 inches). The amount of siderite was varied between 0.5 and 5.0 by weight of the amended layer, corresponding to application rates ranging from 0.14 to 2.84 lbs of siderite per square-foot of cap area (lbs/sq.-ft).

In the cap model, the upper boundary condition is represented by a fixed concentration boundary condition with chemical concentrations characteristic of Onondaga Lake water (Table 3). The lower boundary condition is a time-varying flow and concentration boundary representing ILWD hyperalkaline porewater. The average of porewater analyses for PW-1 and PW-2 reported in SSPA (2009) was used to set concentrations. Hyperalkaline porewater was allowed to advect through the column at a rate of 2 cm/yr (0.066 ft/yr) (SSPA 2008a). The model also included an additional advective flux component to account for porewater expression during cap

consolidation. Estimates for the porewater expression flux during cap consolidation were provided by Geosyntec (2009). The cumulative porewater flux used to model the porewater flow rate through the cap during the first 30 years after cap construction is shown in Figure 7.

The pH of porewater flowing into the cap layer was allowed to change over time from an initial value of 12 to a final value of 11. This change in pH represents the expected shift in porewater pH over time as the current porewater volume is flushed out of the ILWD, and is replaced by porewater that is buffered by the solid phases present in ILWD[3]. The final ILWD porewater pH of 11 is based on previous mineralogical and equilibration studies conducted on ILWD (SSPA, 2008b). Detailed examination of several cores from locations within the ILWD exhibiting the highest porewater pH revealed an absence of solid phases that could presently buffer the pH at values of 12 or greater (i.e. calcium hydroxide), indicating that such phases, which may have been initially present in the waste deposits, have been completely dissolved, and are not presently buffering the pH of the ILWD porewater. Furthermore, sequential equilibration tests indicated that the solid phases present in ILWD would naturally buffer porewater pH to values near 11.

Finally, the chemical reactions required to model the batch test pH evolution curves obtained from the batch tests (equilibrium speciation of ions, kinetic dissolution of siderite, equilibrium precipitation of goethite, and kinetic precipitation of calcite) were included within the sediment cap.

3.2 Model Scenarios

Simulations were performed for a range of siderite amendment mass application rates and for two amendment layer thicknesses in order to determine minimum siderite amendment rates required to achieve both effective pH neutralization and sufficient long-term capacity.

In evaluating the amendment mass requirement for effective porewater pH neutralization by a granular siderite-amended cap, two factors need to be considered. These are:

1) Initiation period – How long after cap construction will it take for the porewater exiting the amended layer to reach a pH of 8 or less?

[3] The shift in porewater pH was simulated by setting the location of the lower model boundary to a depth of 5 feet below the base of the cap, and changing the initial pH value at this boundary from 12 to 11 at a model time of 50 years. A gradual change in pH was thus achieved at the base of the cap due to advective-diffusive transport during the estimated advective travel time of 75 years (from the lower boundary to the amended layer). No chemical reactions were allowed within this portion of the model domain.

2) Longevity – For what period of time after cap construction will the amendment be effective at controlling porewater pH to a value of 8 or less?

The first factor is potentially performance-limiting if pH neutralization is slower than the residence time of porewater in the amended layer. This would be most likely to occur during the rapid porewater expulsion associated with cap consolidation (Figure 7). Thus, one set of model simulations was performed using the slowest rate for granular siderite dissolution reported in Table 2 (GS6). Output from the model included porewater pH at the top of the amended layer as a function of time. The porewater pH curves predicted from these simulations represent a conservative (worst case) estimate of effluent pH during cap consolidation.

A second set of simulations was performed to assess cap longevity. For these simulations, siderite was allowed to instantaneously dissolve to its equilibrium solubility in the porewater. This is conservative because it would represent the maximum possible dissolution of siderite per unit time and thus the fastest amendment mass depletion rate. Model simulations were performed for a period of 2,000 years to evaluate longevity. Output from the model included porewater pH at the top of the amended layer, and the amount of siderite remaining in the cap as a function of time.

3.3 Cap Initiation Period

The simulated porewater pH evolution curves for 3-inch thick siderite-amended layer are shown in Figure 8a. The model results indicate that pH would not be neutralized to a value below 8 during the first several months following cap construction. The initiation time before cap porewater pH attains values less than 8 ranges from approximately 5 months for an application rate of 1% granular siderite (0.28 lb/sq.-ft) to approximately 2 months for an application rate of 5% (1.42 lb/sq.-ft).

In contrast to these results, no initiation time is predicted for the case of a 6-inch thick amended layer (Figure 8b). This difference is largely due to the longer flow path and contact time between siderite and porewater. Porewater pH is initially predicted to decreases below 7 at early times (<3 months) at the top of the amended layer due to goethite precipitation prior to the arrival of the initial ILWD porewater flux.

3.4 Cap Longevity

Because amendment longevity was simulated by assuming instantaneous (equilibrium) reaction between porewater and granular siderite, the thickness of the amended layer does not affect

model predictions. In this case, granular siderite in the first modeled grid cell that encounters hyperalkaline porewater will instantaneously dissolve to equilibrium. Once siderite has been completely depleted in this grid cell, the neutralization reaction shifts to the next cell along the flowpath of ILWD porewater. The insensitivity of model predictions to amended layer thickness is illustrated in Figure 9, which shows predicted amendment longevity as a function of siderite mass application rate for 3 inch and 6 inch amendment layer thicknesses. As shown in the figure, the only factor determining cap longevity is the amendment mass application rate.

The simulated porewater pH evolution and siderite mass depletion curves for a range of amendment application rates are shown in Figures 10a and 10b, respectively. In order to achieve a longevity of 1,000 year, a siderite mass application rate of at least 1 lb/sq-ft is required (corresponding to approximately 3.5 weight % granular siderite in a 3-inch sand layer, or 1.8 weight % in a 6-inch sand layer).

4 Conclusions and Recommendations

Results of cap modeling indicate that both short and long-term cap effectiveness requirements for porewater pH control would be met with a mass application rate of granular siderite of 1.0 lb/sq-ft mixed with sand in a 6 inch layer. The modeling indicates that emplacement within a 3-inch thick siderite-sand layer may result in a delay of up to several months before porewater pH exiting the amendment layer is buffered to circumneutral values. Although this is a very short duration in comparison to the expected cap lifetime and does not impact the long-term effectiveness of the cap, modeling results also indicate that emplacement of amendment in a 6-inch (or thicker) layer would circumvent the initial delay in performance.

One potentially critical implication of the predicted mass application rate is in relation to the physical distribution of siderite particles at the pore-scale within the amended layer. Pore-scale mass transfer limitations on reactions in porous media become more important for solid phases present at low to trace levels. A mass application rate of 1 lb/sq-ft equates to less than 2% by weight within a 6-inch layer. In this configuration, some porewater flow pathways will be exposed to less siderite than others, such that the average extent of reaction across the amendment layer may be less than predicted by the model. The effect of pore-scale heterogeneity on the performance of the amendment layer at field scale cannot be addressed with the present model.

To address this issue, we recommend a focused column test study to confirm the predicted pH neutralizing performance in a properly scaled dynamic porous medium setting. The column test

results would be used to update the cap pH model, thereby providing an increased level of confidence in the predicted long-term performance and the optimization of design parameters for the amended cap.

5 References

Duckworth, O.W. and S.T. Martin (2004) Role of molecular oxygen in the dissolution of siderite and rhodocrosite. G*eochim. Cosmochim. Acta* 68:607-621.

Geosyntec (2009) Predicted Cumulative Sediment Cap Consolidation Data.

Kinniburgh, D.G., and D.M. Cooper (2009) PhreePlot: Creating graphical output with PHREEQC. Available online at: http://www.phreeplot.org. Accessed March, 2009.

Lebron, I., and D.L. Suarez (1996) Calcite nucleation and precipitation kinetics as affected by dissolved organic carbon. G*eochim. Cosmochim. Acta* 60:2765-2776.

Lin, Y.-P. and P.C. Singer (2005) Effects of seed material and solution composition on calcite precipitation. G*eochim. Cosmochim. Acta* 69:4495-4504.

Morse, J.W., R.S. Arvidson, and A. Lüttge (2007) Calcium carbonate formation and dissolution. *Chem. Rev.* 107:342-381.

Palandri, J., and Y.K. Kharaka (2004) A compilation of rate parameters of water-mineral interaction kinetics for application to geochemical modeling. USGS Open-File Report 2004-1068, 64 pp.

Parkhurst, D.L., and C.A.J. Appelo (1999) User's guide to PHREEQC (Version 2)—a computer program for speciation, batch-reaction, one-dimensional transport, and inverse geochemical calculations. USGS Water-Resources Investigations Report 99-4259, 312 pp.

Pokrovsky, G.S. and J. Schott (2002) Surface chemistry and dissolution kinetics of divalent metal carbonates. *Environ. Sci. Technol.* 36:426-432.

Schott, J., O.S. Pokrovsky, and E.H. Oelkers (2009) The link between dissolution/precipitation kinetics and solution chemistry. *In* Reviews in Mineralogy and Geochemistry (Oelkers and Schott, *eds.*), V. 70, p. 207-258.

S.S. Papadopulos & Associates (2008a) Preliminary Evaluation of Upwelling Velocities from Phase III: Addendum 5 Geoprobe and Vibracore Data. Memorandum dated April 11.

S.S. Papadopulos & Associates (2008b) SMU-1 Hyperalkaline pH Source Identification and Neutralization Evaluation. Memorandum dated July 30.

S.S. Papadopulos & Associates (2009) ILWD Porewater pH Neutralization Batch Studies. Memorandum dated September 22.

Attachments

Tables

Figures

Appendix A PHREEQC Model Files for Sediment Cap Porewater pH Model

Table 1. Summary of Batch Test Experimental Conditions

Amendment[1]	Experiment	Solution	L/S[2]
Powdered Siderite (unrinsed)	S1	PW-1	12.5
	S2		12.5
	S3	PW-2	2.5
	S4		12.5
	S5		50.0
Pelletized Siderite (unrinsed)	PS1	PW-1	12.5
	PS2		12.5
	PS3	PW-2	2.5
	PS4		12.5
	PS5		50.0
Pelletized Siderite	PS6	PW-3	5
	PS7		
Granular Siderite (bulk)	GS1	PW-3	2.5
	GS2		
	GS3		5
	GS4		
	GS5		10
	GS6		
Granular Siderite (1-2 mm)	GS7		5
	GS8		10
Granular Siderite (0.5-1 mm)	GS9		5
Granular Siderite (0.25-0.5 mm)	GS10		5
Granular Siderite (0.125-0.25 mm)	GS11		10

Notes: [1]Amendments were rinsed to remove fines prior to batch testing unless otherwise indicated.

[2]L/S = liquid to solid-amendment ratio

Table 2. Optimized Kinetic Parameters for pH Neutralization

Amendment[1]	Experiment	Solution	L/S	Siderite						Calcite		R^2
				k_s mol/g/s	k_{sb} mol/g/s	n_b	k_{sf} mol/g/s	m_s grams	Fraction Fines (%)[2]	k_c mol/s	n_c[3]	
Powdered Siderite (unrinsed)	S1, S2	PW-1	12.5	4.42×10^{-11}	1.55×10^{-22}	-1	2.77×10^{-7}	68	0.30	1.05×10^{-9}	0.14	0.998
	S3	PW-2	2.5	2.40×10^{-11}	3.25×10^{-22}	-1	1.06×10^{-6}	337	0.01	8.49×10^{-10}	0.30	0.982
	S4		12.5	3.35×10^{-11}	1.03×10^{-22}	-1	--[4]	68	0.00	2.69×10^{-10}	0.25	0.986
	S5		50	1.04×10^{-11}	3.87×10^{-22}	-1	1.25×10^{-6}	17	0.87	3.58×10^{-10}	0.23	0.992
Pelletized Siderite (unrinsed)	PS1, PS2	PW-1	12.5	1.07×10^{-13}	3.45×10^{-23}	-1	1.23×10^{-7}	61	0.95	5.09×10^{-11}	0.40	0.995
	PS3	PW-2	2.5	7.83×10^{-12}	5.51×10^{-21}	-1	--[4]	307	0.00	1.02×10^{-10}	0.16	0.996
	PS4		12.5	7.90×10^{-12}	7.71×10^{-22}	-1	1.00×10^{-6}	63	0.09	2.36×10^{-10}	0.27	0.986
	PS5		50	3.51×10^{-13}	1.02×10^{-21}	-1	5.72×10^{-7}	18	1.24	1.78×10^{-10}	0.34	0.872
Pelletized Siderite	PS6	PW-3	5	5.21×10^{-12}	7.46×10^{-21}	-1	NA[5]	152	NA[5]	3.51×10^{-10}	0.24	0.996
	PS7			5.38×10^{-12}	7.63×10^{-21}	-1	NA[5]	152	NA[5]	2.35×10^{-10}	0.30	0.995
Granular Siderite (bulk)	GS1	PW-3	2.5	3.48×10^{-11}	6.07×10^{-22}	-1	NA[5]	344	NA[5]	9.52×10^{-10}	0.25	0.991
	GS2			2.18×10^{-11}	6.68×10^{-22}	-1	NA[5]	332	NA[5]	9.81×10^{-10}	0.27	0.999
	GS3		5	1.99×10^{-12}	4.07×10^{-22}	-1	NA[5]	168	NA[5]	5.41×10^{-10}	0.23	0.995
	GS4			5.51×10^{-12}	5.57×10^{-22}	-1	NA[5]	169	NA[5]	5.81×10^{-10}	0.22	0.998
	GS5		10	3.87×10^{-12}	2.42×10^{-22}	-1	NA[5]	84	NA[5]	4.27×10^{-10}	0.22	0.995
	GS6			1.83×10^{-12}	2.32×10^{-22}	-1	NA[5]	84	NA[5]	4.24×10^{-10}	0.21	0.994
Granular Siderite (1-2 mm)	GS7		5	2.47×10^{-11}	9.33×10^{-22}	-1	NA[5]	164	NA[5]	6.04×10^{-10}	0.22	1.000
	GS8		10	2.15×10^{-12}	5.93×10^{-22}	-1	NA[5]	83	NA[5]	3.34×10^{-10}	0.27	0.987
Granular Siderite (0.5-1 mm)	GS9		5	3.37×10^{-11}	7.75×10^{-22}	-1	NA[5]	169	NA[5]	9.96×10^{-10}	0.20	0.998
Granular Siderite (0.25-0.5 mm)	GS10		5	5.25×10^{-11}	1.24×10^{-21}	-1	NA[5]	167	NA[5]	1.82×10^{-09}	0.17	0.975
Granular Siderite (0.125-0.25 mm)	GS11		10	1.39×10^{-11}	2.31×10^{-21}	-1	NA[5]	89	NA[5]	8.79×10^{-10}	0.15	0.994

Notes: [1]Amendments rinsed prior to batch testing unless otherwise indicated

[2]Fraction of fines (%) calculated from $100 \times (m_{sf}/m_s)$.

[3]Fitted values for n_c ranged from 0.14 to 0.40, consistent with Lin and Singer (2005), who report values <1 for "natural" mineral surfaces.

Table 3. Model Input Parameters for Siderite-Amended Sediment Cap Simulations

Parameter Group	Parameter	ILWD[1]	Cap (initial)[2]	Onondaga Lake[2]	Units
Transport[3]	Flow Rate	2.0	2.0[4]	NA	cm/yr
	Diffusivity	6×10^{-6}	6×10^{-6}	NA	cm^2/s
	Dispersivity	6	6	NA	cm
	Porosity	0.3	0.3	NA	-
Initial Water Chemistry	Temperature	11	11	11	deg. C
	pH	12.0	7.0	7.0	-
	Dissolved Oxygen	0.0	1.5	1.5	mg/L
	Alkalinity[5]	1440	10.7	10.7	mg/L
	Calcium	5780	59.2	59.2	mg/L
	Potassium	282	4.2	4.2	mg/L
	Magnesium	0	22.8	22.8	mg/L
	Sodium	8460	193	193	mg/L
	Chloride[6]	25100	359	359	mg/L
	Sulfate	280	144	144	mg/L

Notes:

[1]Initial water chemistry for ILWD porewater based on average of PW-1 and PW-2 unless otherwise indicated.

[2]Data from SSPA, 2008a. Cap assumed to be initially saturated with lake water.

[3]The column height of 5 feet was discretized into either 450 cells for initiation time simulations or 150 cells for longevity simulations.

[4]Nominal value. Additional time-dependent porewater expression due to cap settlement was also included in the model (see text for additional explanation).

[5]Model-calculated value.

[6]Chloride concentrations were adjusted slightly from reported values to achieve charge balance.

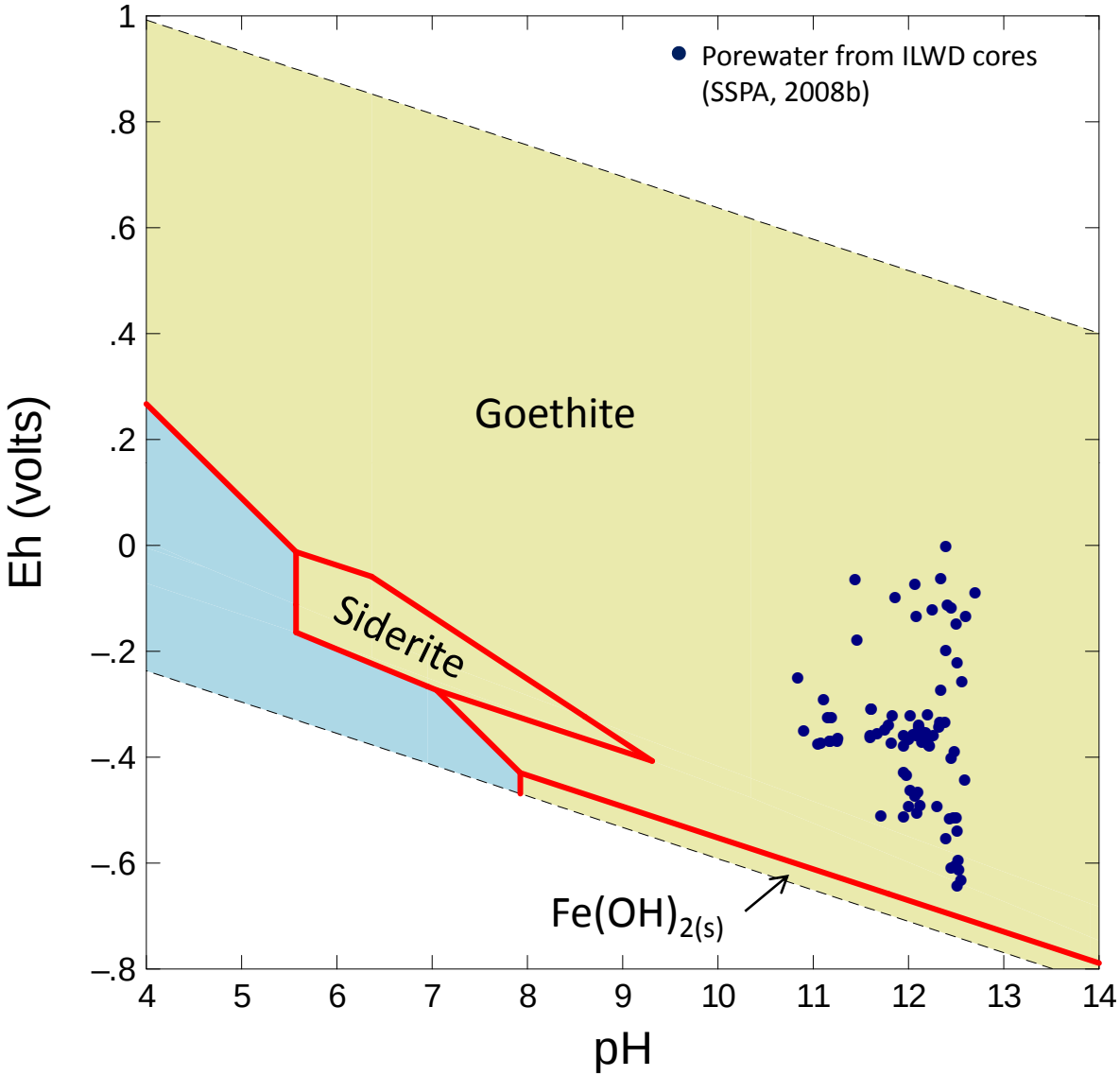

Figure 1. Eh-pH diagram showing conditions measured in ILWD porewater in relation to stability fields of goethite and other iron phases.

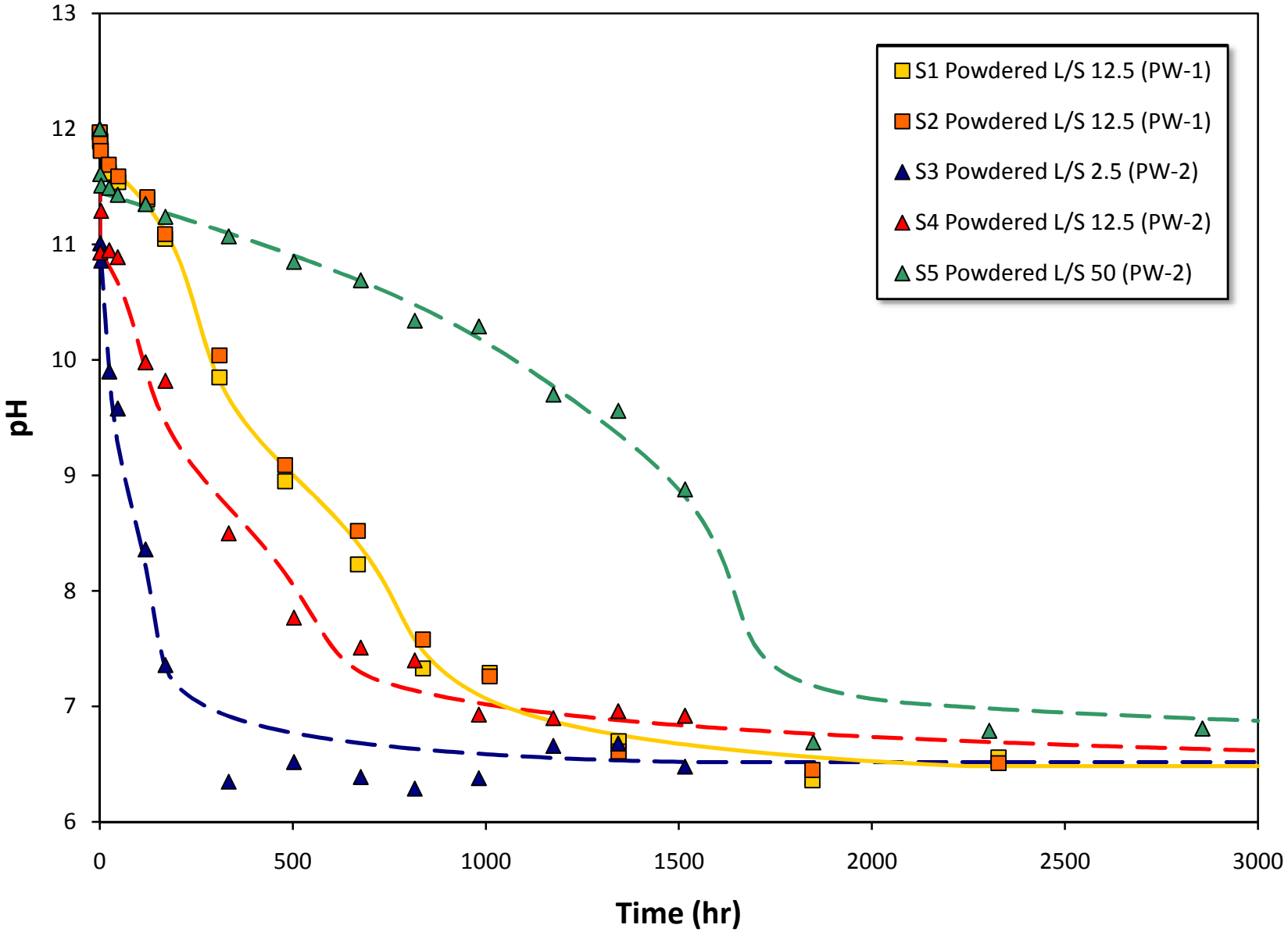

Figure 2. Measured (symbols) and predicted (lines) solution pH as a function of time in powdered siderite batch tests.

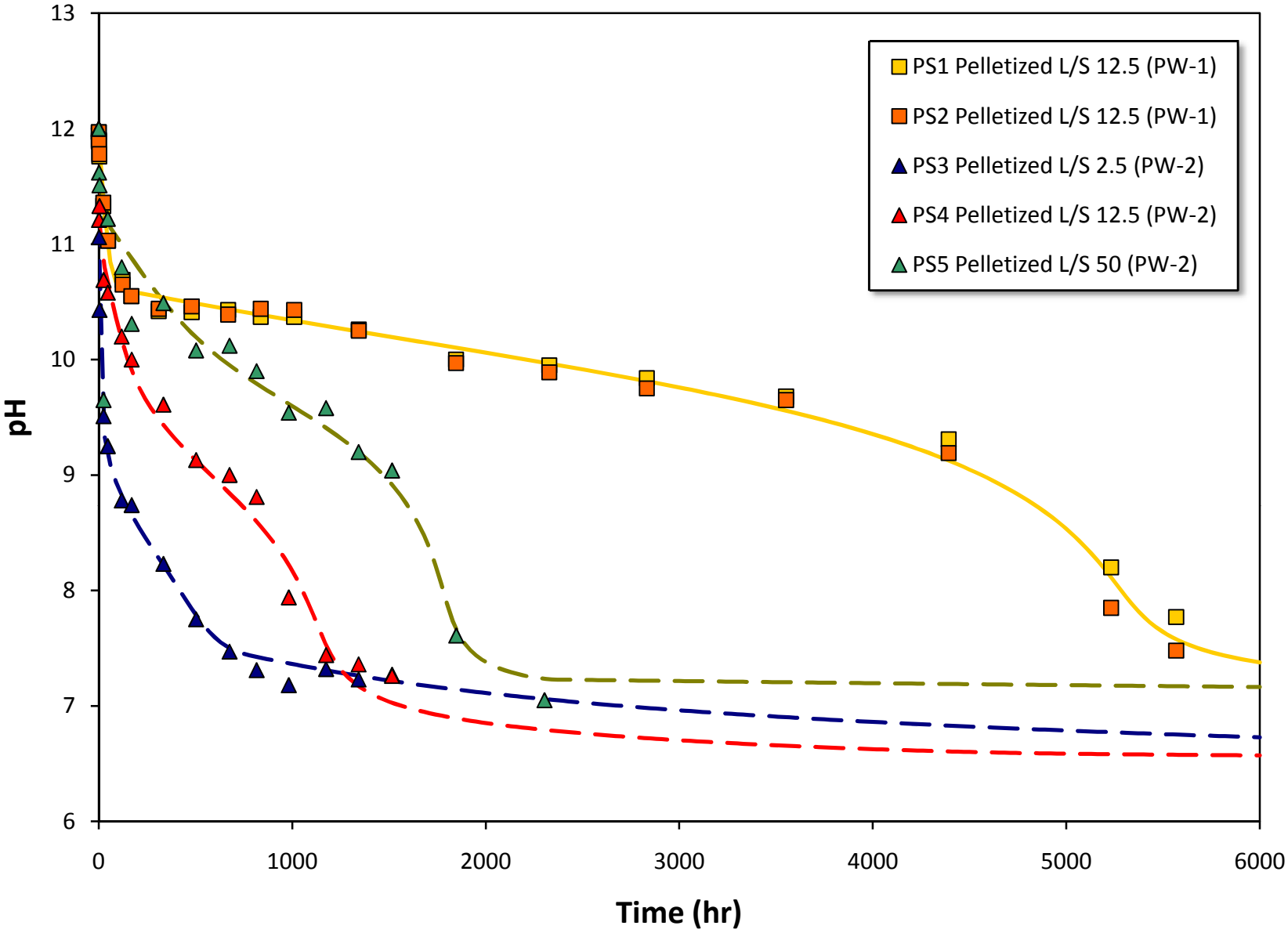

Figure 3a. Measured (symbols) and predicted (lines) solution pH as a function of time for unrinsed pelletized siderite batch tests.

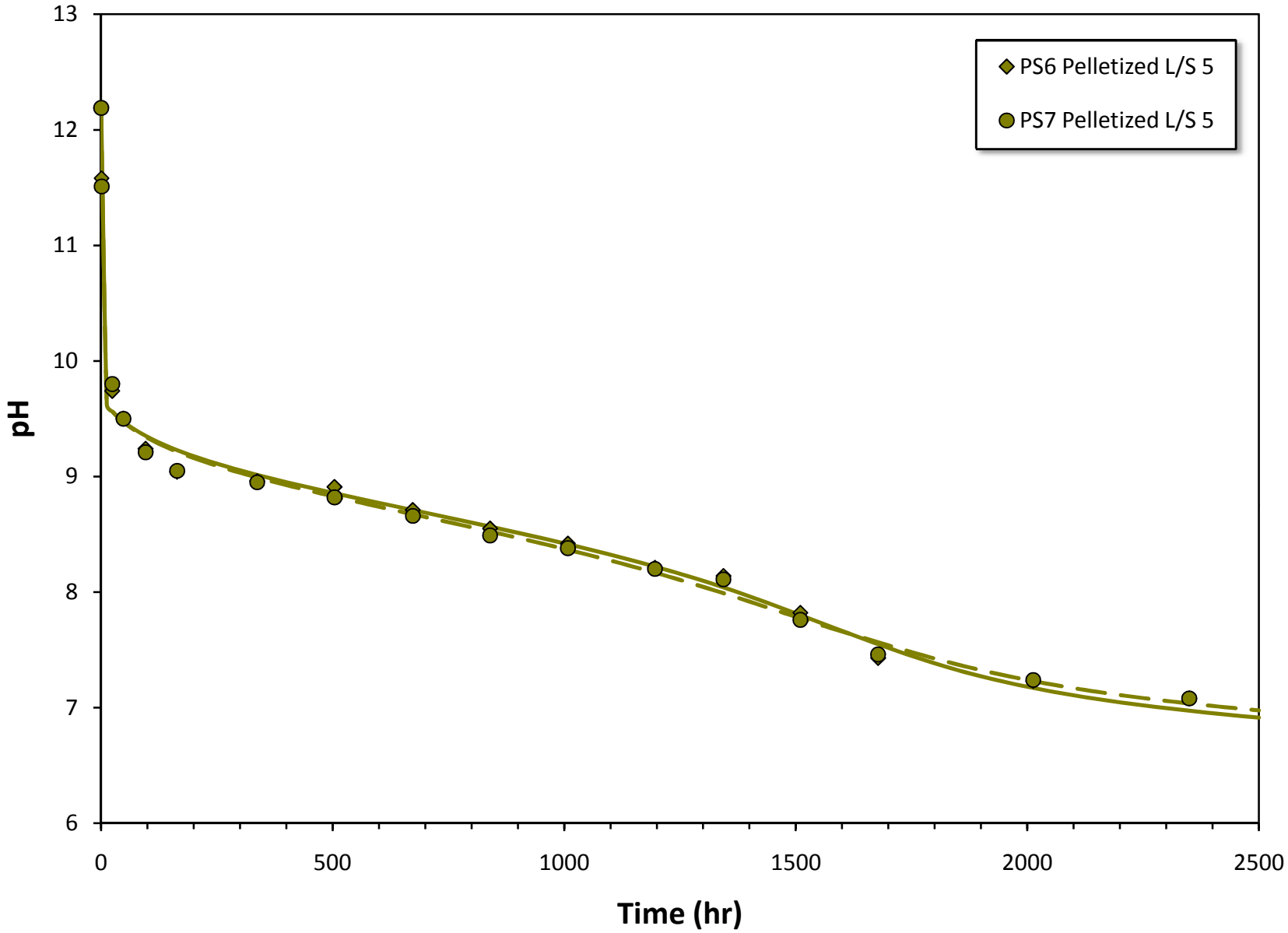

Figure 3b. Measured (symbols) and predicted (lines) solution pH as a function of time for rinsed pelletized siderite batch tests at L/S = 5.

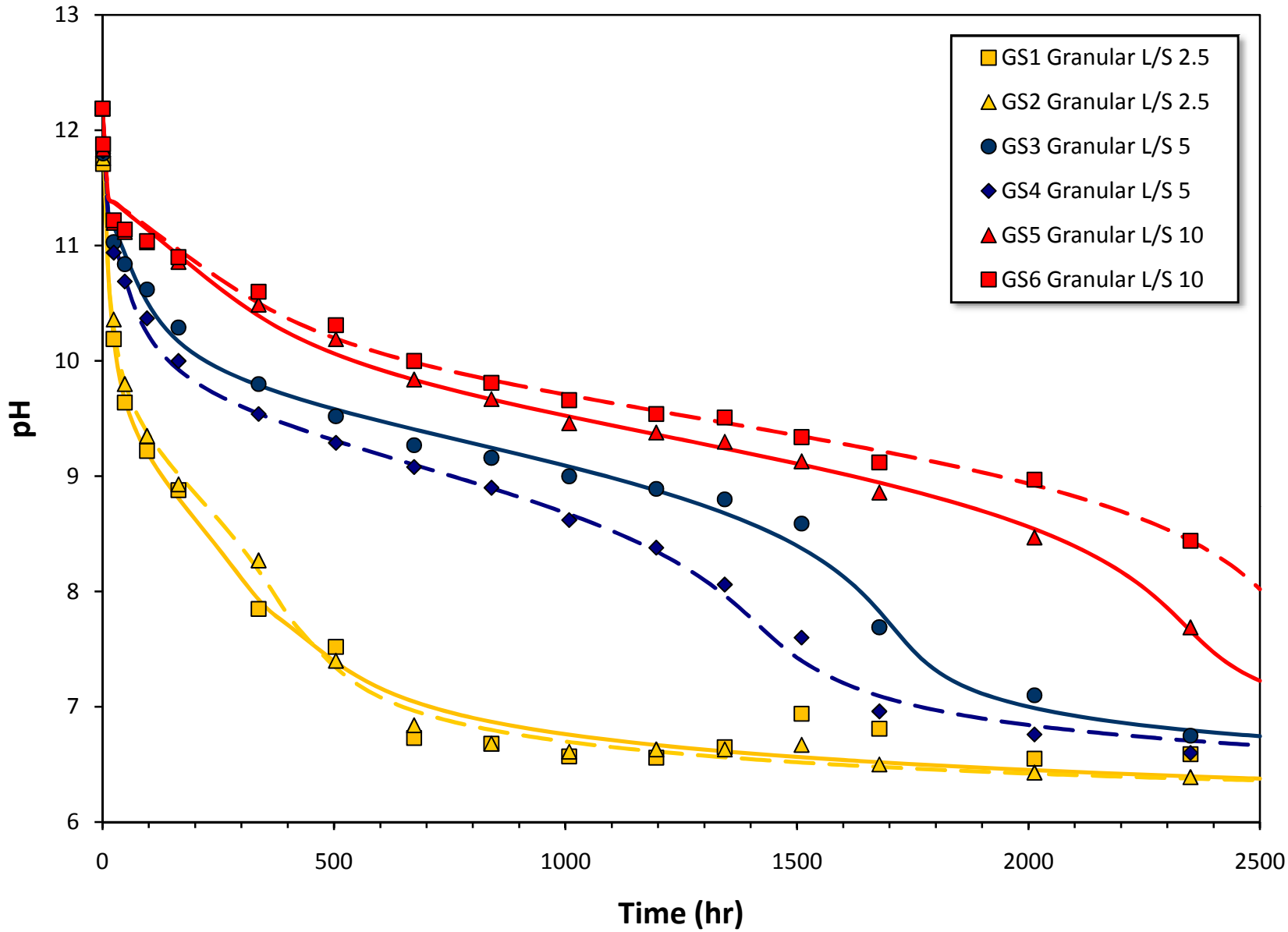

Figure 4a. Measured (symbols) and predicted (lines) solution pH as a function of time for bulk granular siderite batch tests.

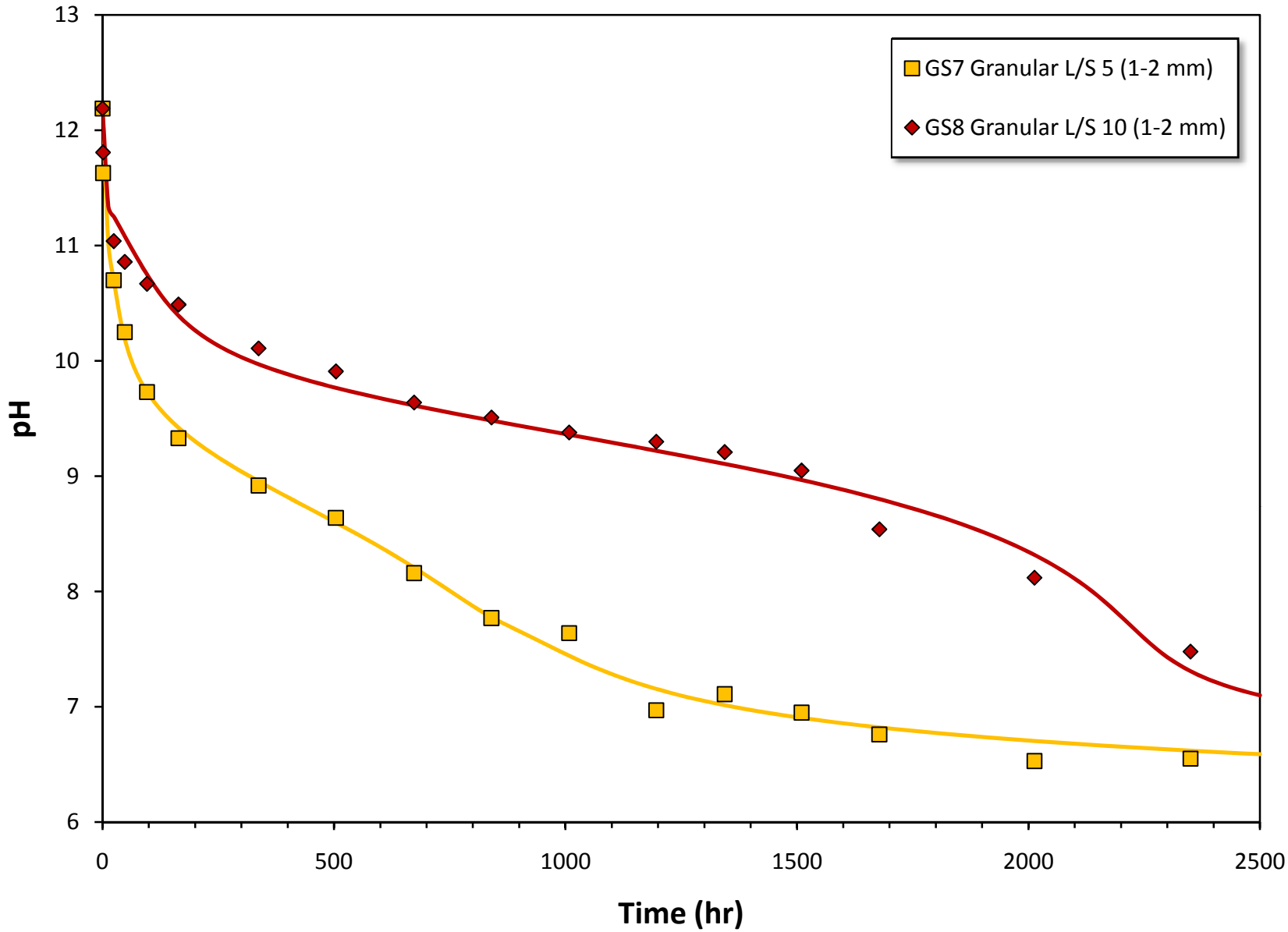

Figure 4b. Measured (symbols) and predicted (lines) solution pH as a function of time for granular siderite (1-2 mm grain-size fraction) batch tests.

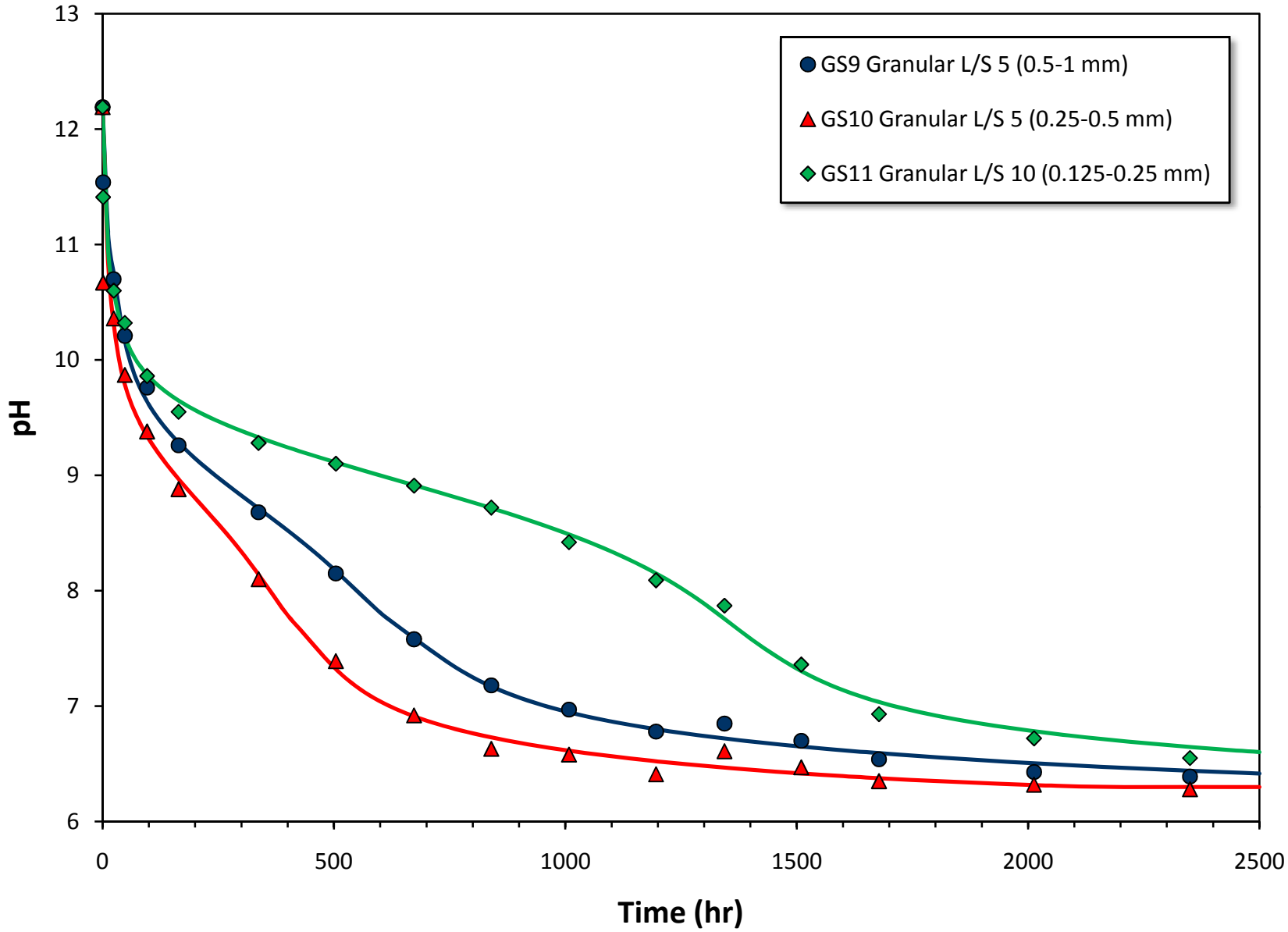

Figure 4c. Measured (symbols) and predicted (lines) solution pH as a function of time for finer grain-size fractions granular siderite batch tests.

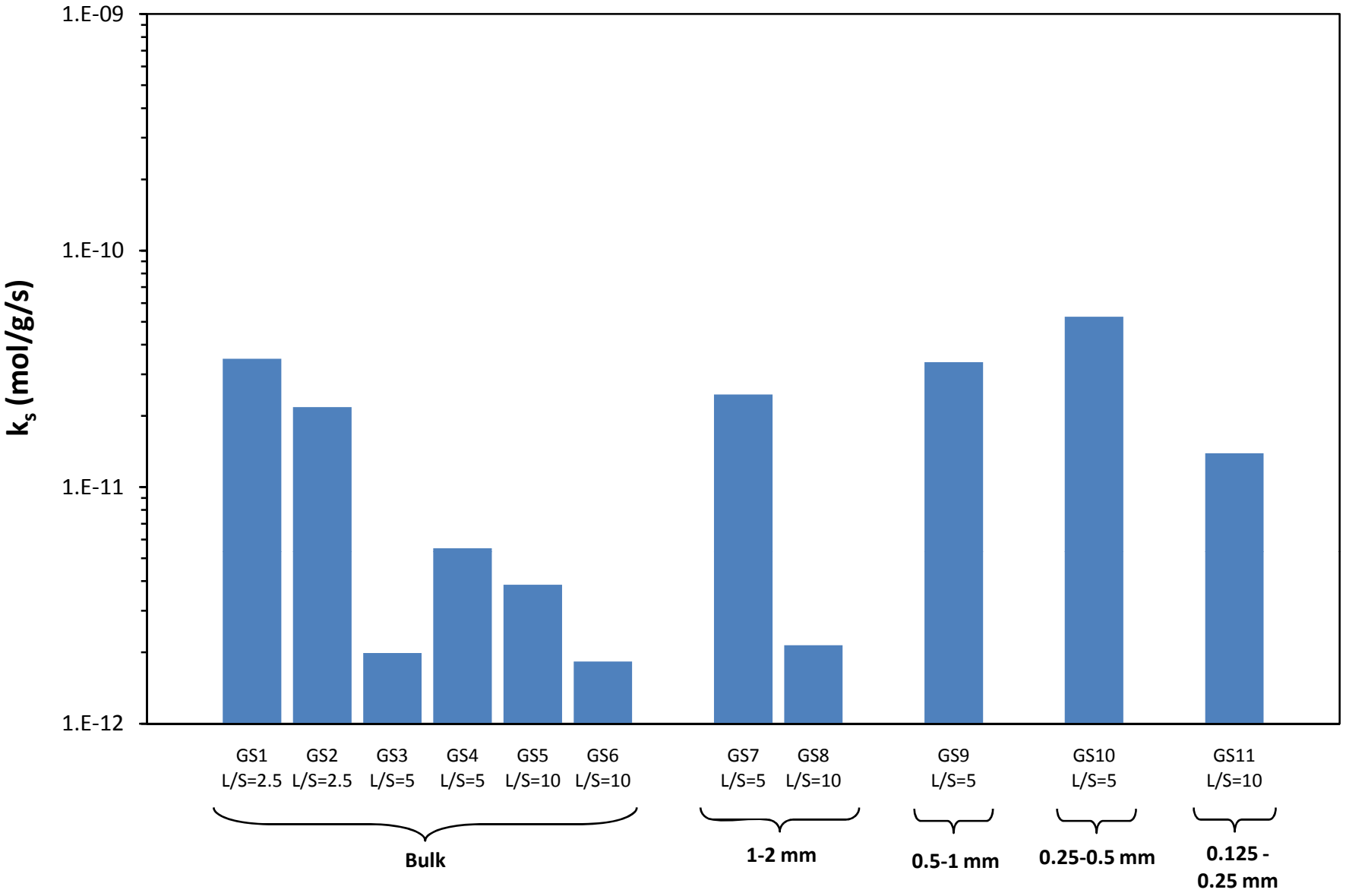

Figure 5a. Comparison of fitted pH-independent siderite dissolution rate constants [k_s] (mol/g/s) for granular siderite batch tests as a function of L/S ratio and grain size.

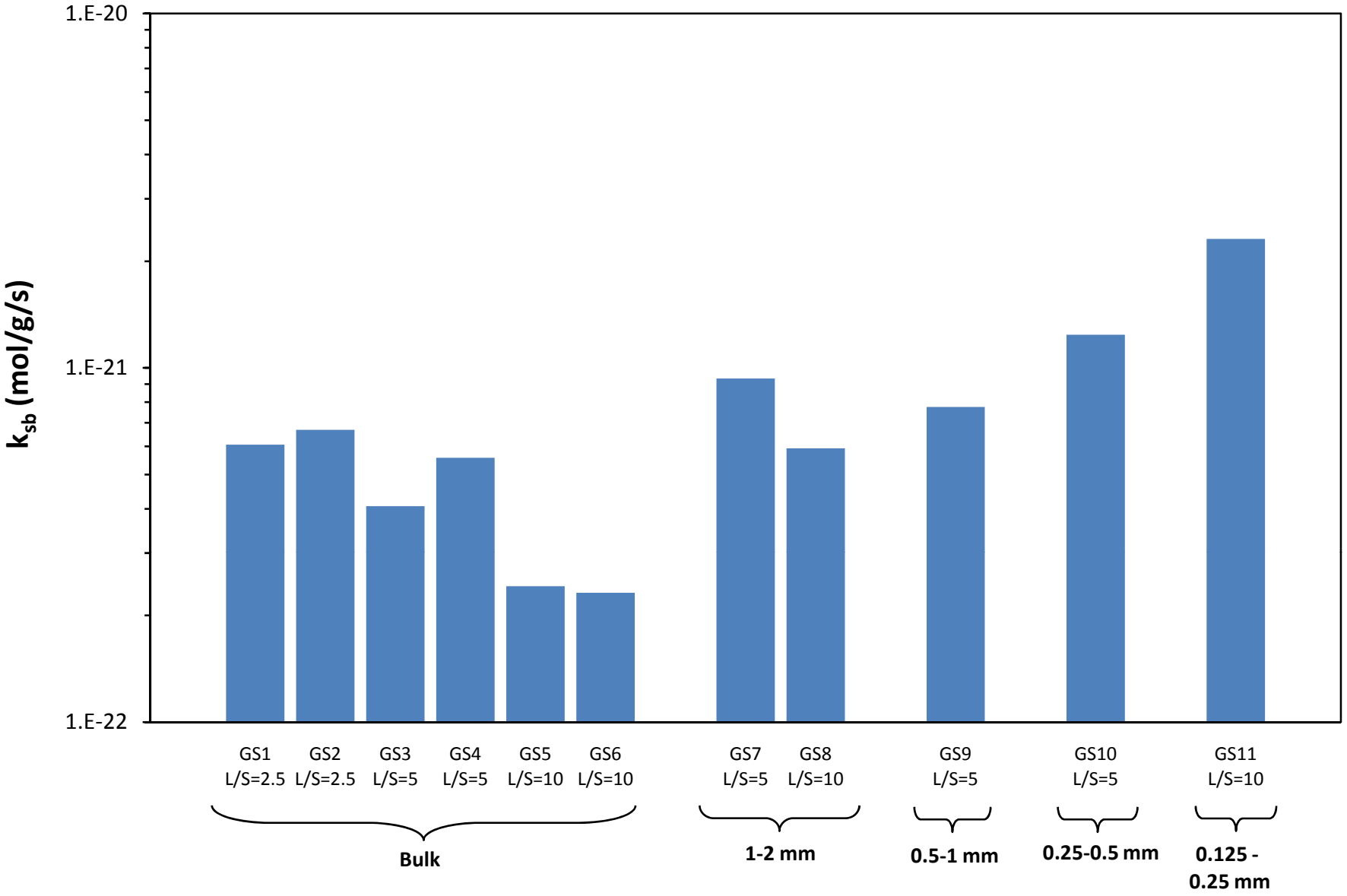

Figure 5b. Comparison of fitted siderite dissolution pH-dependent base mechanism rate constants [k_{sb}] (mol/g/s) for granular siderite as a function of L/S ratio and grain size.

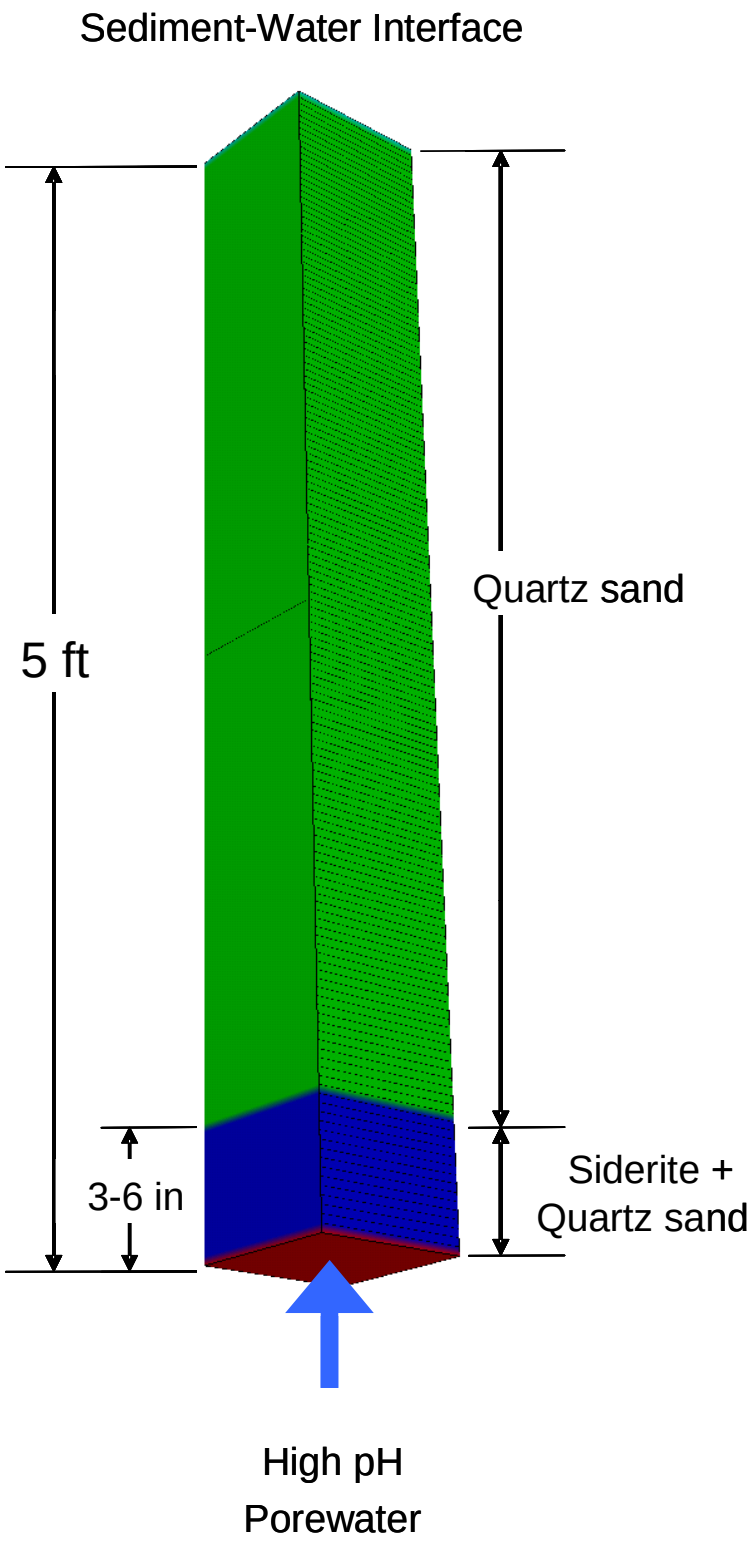

Figure 6. Conceptual model for porewater pH simulations in a granular siderite-amended cap.

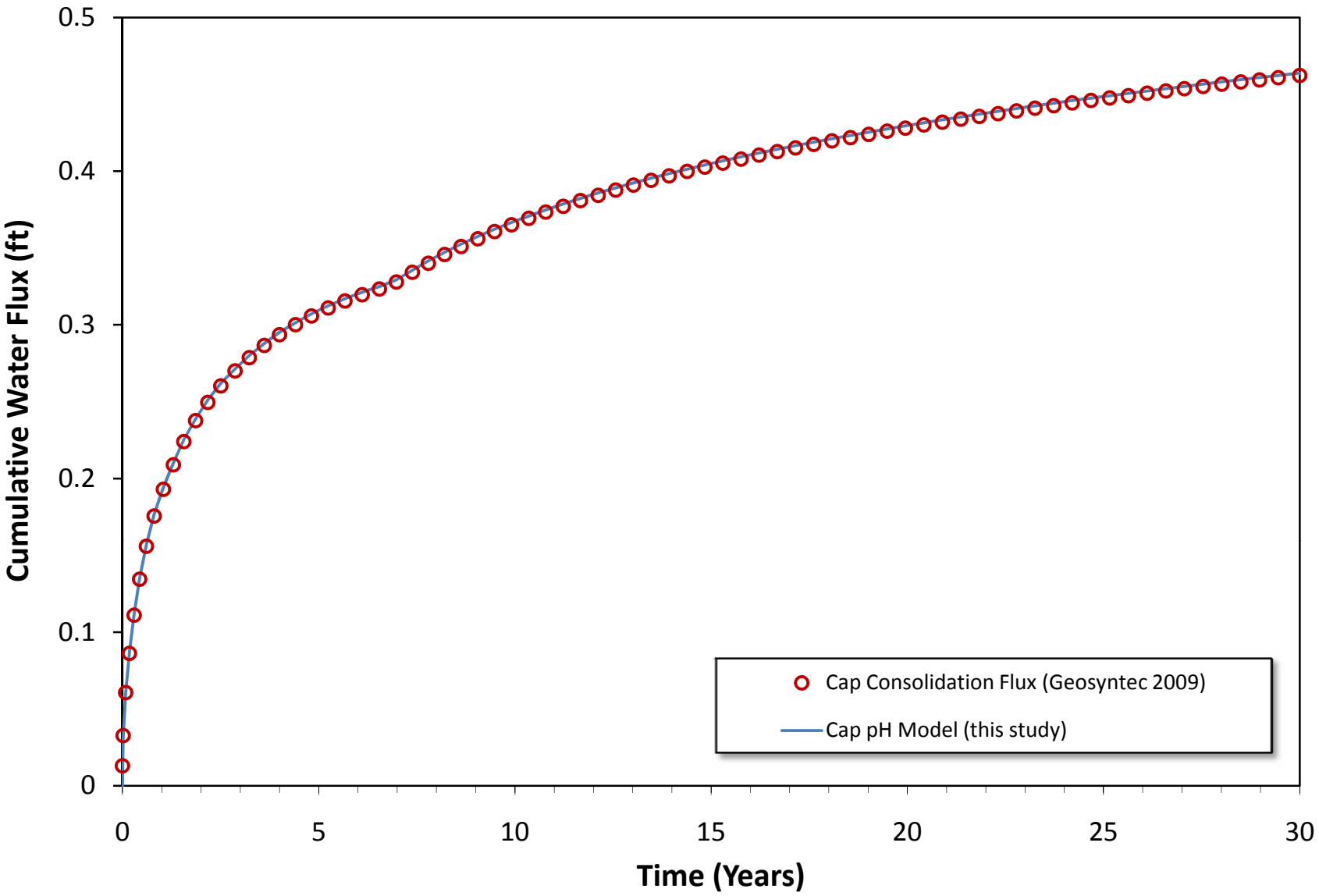

Figure 7. Cumulative upward porewater flux due to cap consolidation.

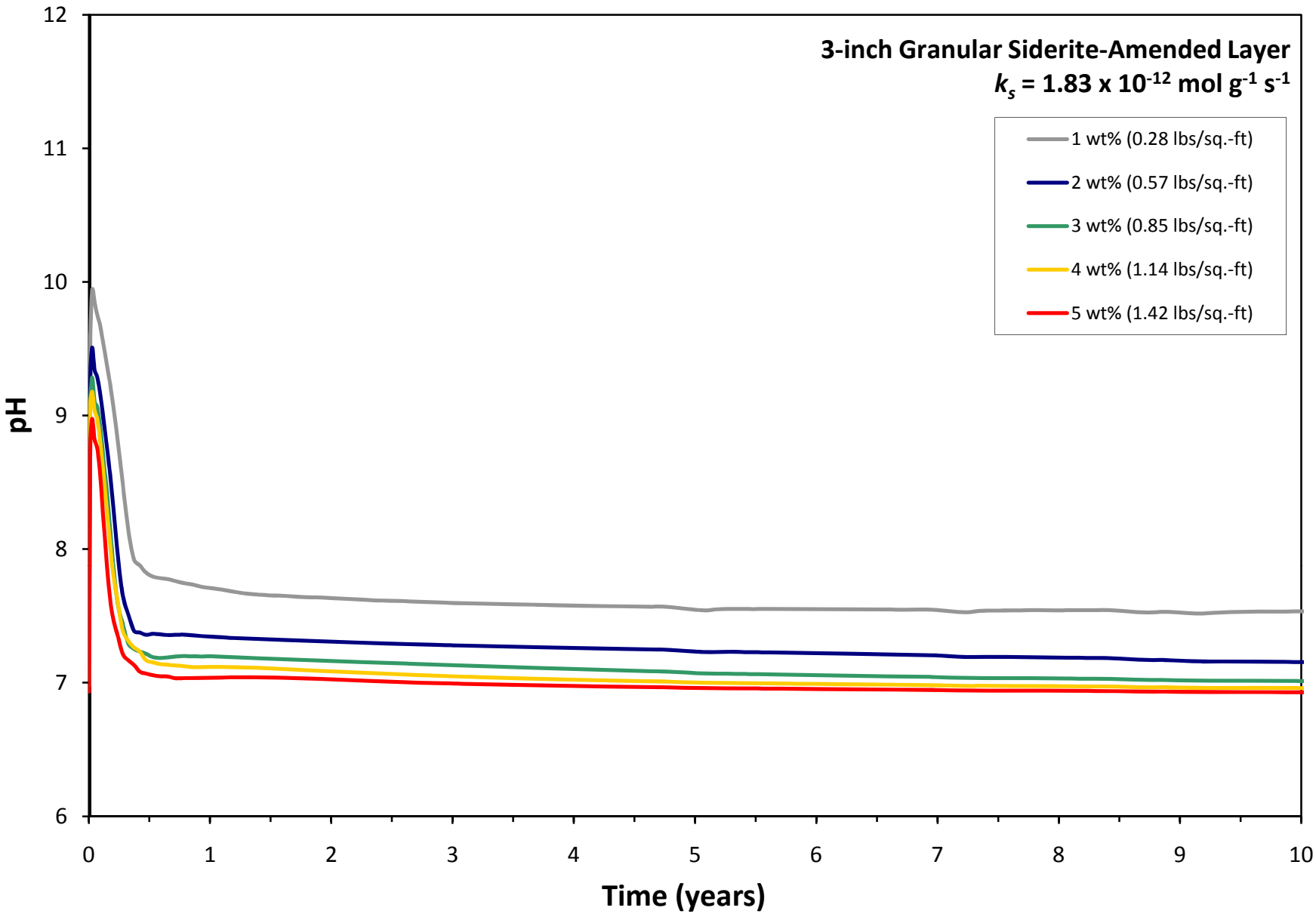

Figure 8a. Predicted porewater pH at the top of a 3-inch thick granular siderite-amended layer.

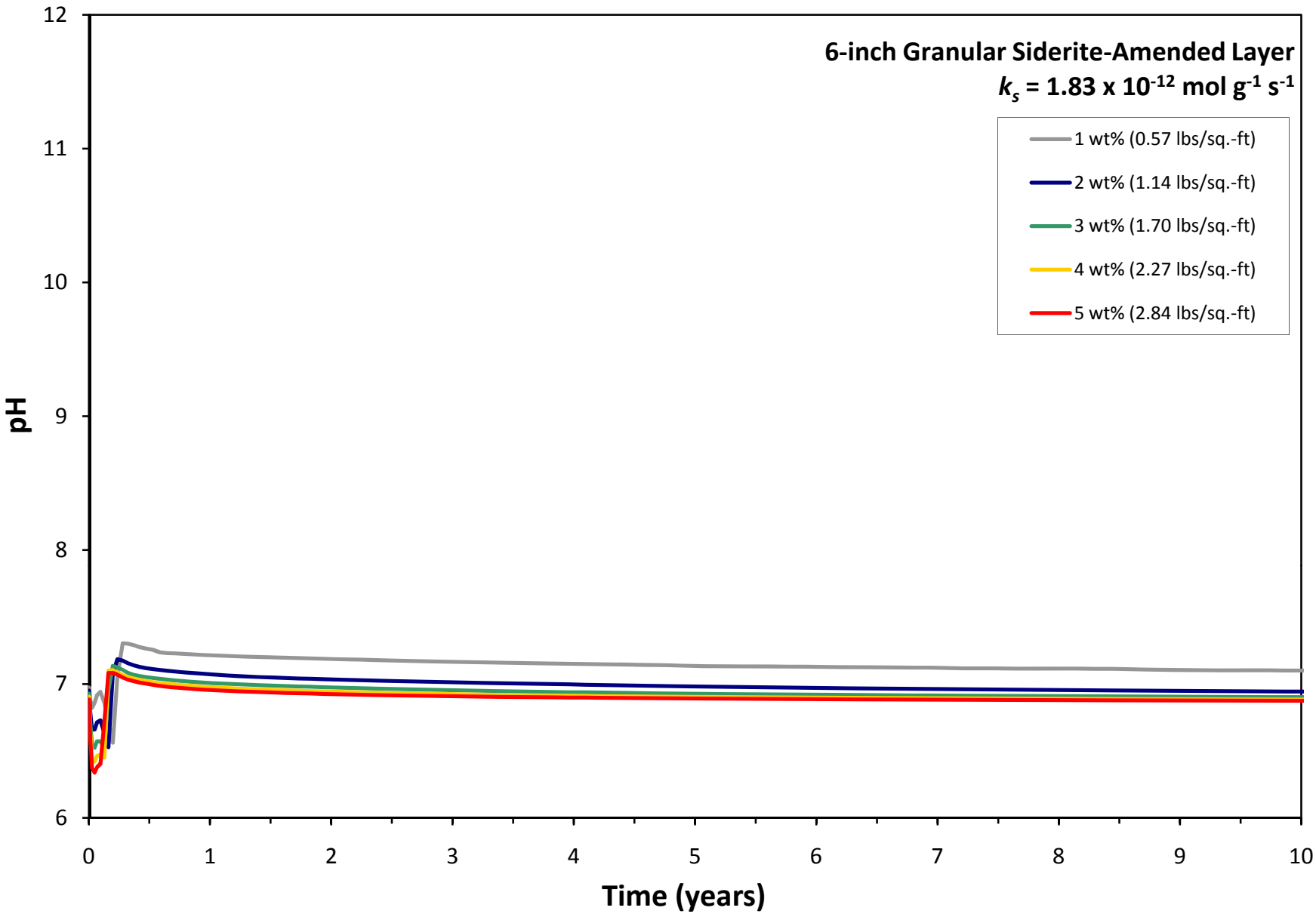

Figure 8b. Predicted porewater pH at the top of a 6-inch thick granular siderite-amended layer.

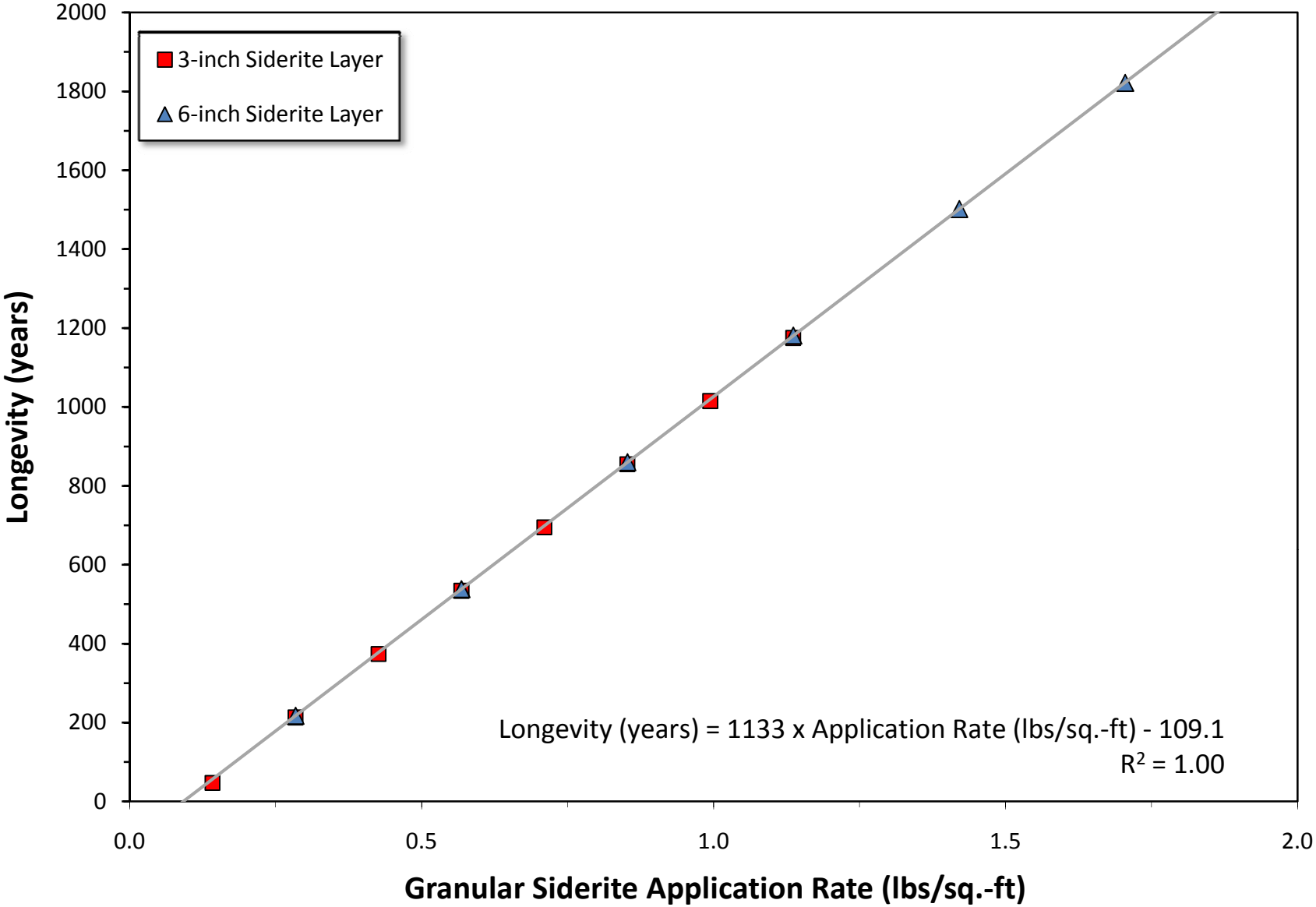

Figure 9. Predicted cap longevity as a function of siderite application rate.

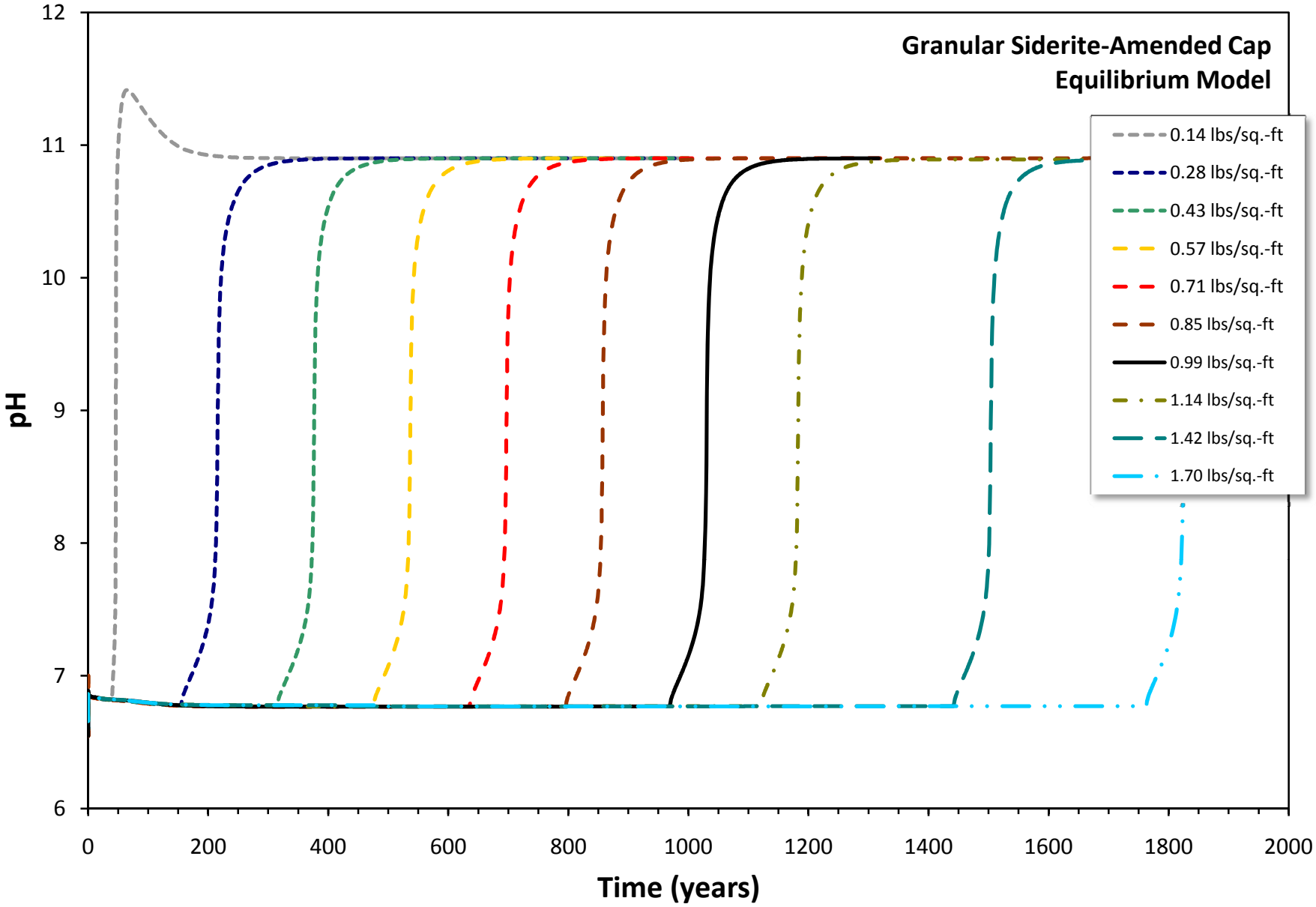

Figure 10a. Predicted porewater pH above the granular siderite-amended layer.

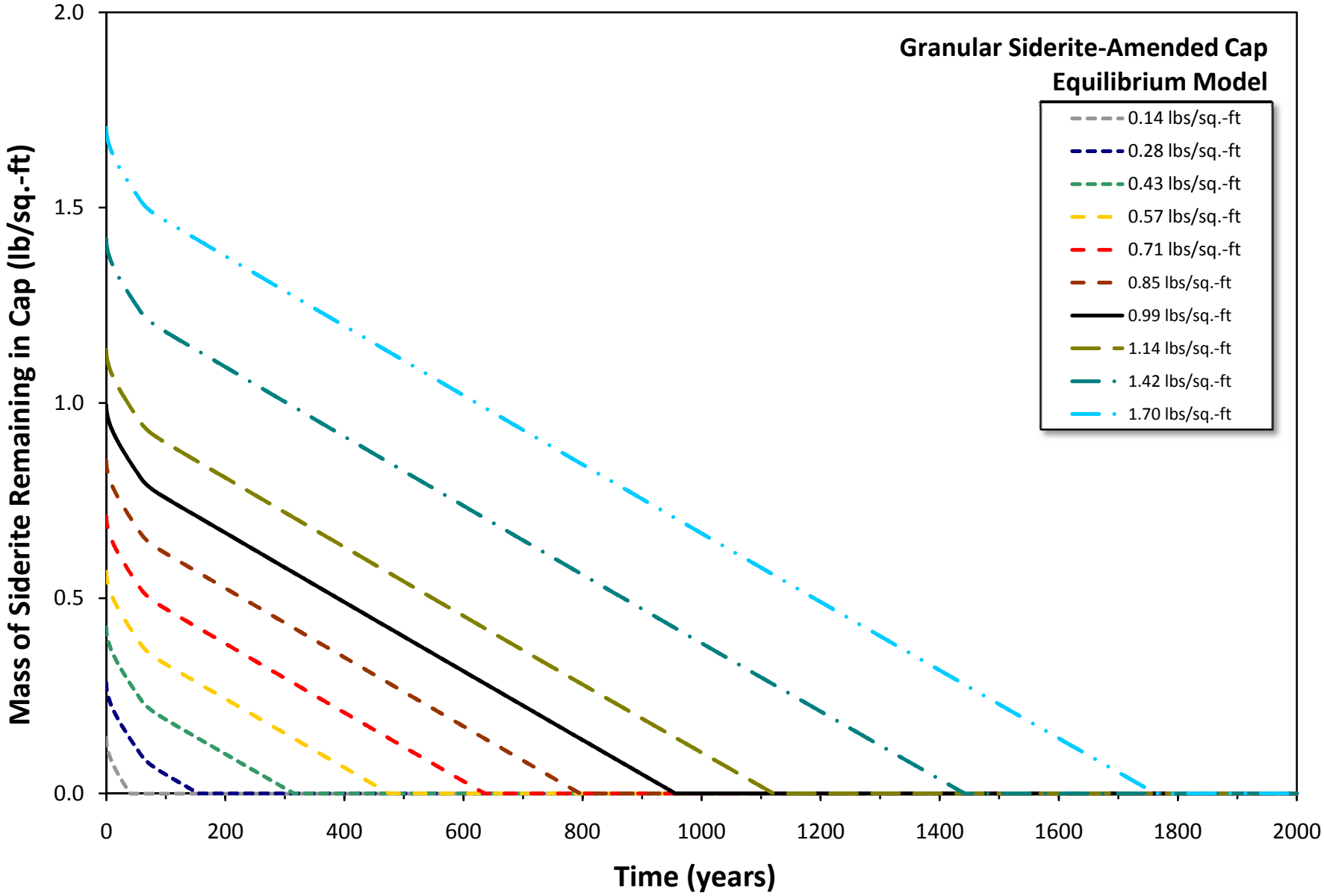

Figure 10b. Predicted depletion of granular siderite in cap as a function of time for different mass application rates.